Project 076 Improved Open Rotor Noise Prediction Capabilities

Georgia Institute of Technology

Project Lead Investigator

Professor Dimitri N. Mavris
Director, Aerospace Systems Design Laboratory
School of Aerospace Engineering, Georgia Institute of Technology
Phone: (404) 894-1557, Fax: (404) 894-6596
Email: dimitri.mavris@ae.gatech.edu

Dr. Jimmy Tai
Division Chief, Propulsion & Energy
Aerospace Systems Design Laboratory
School of Aerospace Engineering, Georgia Institute of Technology
Phone: (404) 894-0197, Fax: (404) 894-6596
Email: jimmy.tai@ae.gatech.edu

University Participants

Georgia Institute of Technology (Georgia Tech)

- P.I.: Dr. Dimitri N. Mavris
- Co-PI: Dr. Jimmy Tai
- FAA Award Number: 13-C-AJFE-GIT-078
- Period of Performance: August 11, 2020 to August 10, 2021
- Task(s):
    - Task 1: Literature review
    - Task 2: Parametric CAD model creation
    - Task 3: Computational aerodynamics analysis (CAA) case setup and validation

Project Funding Level

The project funding is $300,000 per year from the FAA. The cost-share match amount is $300,000 per year. The sources of matching are cash and in-kind cost-sharing from our industry partner (General Electric [GE]).

Investigation Team

- Dr. Dimitri Mavris, Professor, Georgia Tech (P.I.)
- Dr. Jimmy Tai, Senior Research Engineer, Georgia Tech (Co-P.I.)
- Mr. Srujal Patel, Research Engineer II, Georgia Tech
- Dr. Miguel Walter, Research Engineer II, Georgia Tech
- Mr. Christopher Roper, Graduate Student, Georgia Tech
- Mr. Brenton Willier, Graduate Student, Georgia Tech
- Mr. Marcos Dos Santos, Graduate Student, Georgia Tech
- Mrs. Mariam Emara, Graduate Student, Georgia Tech
- Mr. Maxime Varoqui, Graduate Student, Georgia Tech

Project Overview

The contra-rotating open rotor (CROR) system has promising environmental benefits due to its ultra-high bypass ratio and high propulsive efficiency. The reduced fuel burn and emissions of the CROR compared with an equivalent-thrust turbofan

make the CROR a viable economic and environmentally friendly propulsion alternative to traditional ducted systems. However, in the absence of a noise-conditioning duct, aerodynamic interactions within the CROR system as well as between the system and surrounding installation components such as the engine pylon may result in noise penalties. If the system configuration is not optimized, the added effect of flow asymmetry to the aerodynamic interactions could potentially result in severe noise penalties, making the CROR system infeasible for use in the aircraft industry. In the proposed work, a sensitivity study will be performed on the design parameters of a CROR-pylon configuration. This study will leverage knowledge from past efforts with this type of configuration in order to narrow down the space of design parameters. High-fidelity CAA will be carried out to analyze the effect of each of the chosen parameters on noise. This research is intended to provide both the FAA and industry with key insights necessary for design optimization of the CROR system in the future.

Task 1 - Literature Review

Georgia Institute of Technology

Objective(s)

This task is focused on defining a set of design parameters known to affect the aeroacoustics of the open rotor and acknowledged in the open literature. This set will serve as a starting point for further defining a subset of design parameters on which the sensitivity study will be based. Therefore, a literature survey was conducted to summarize the current knowledge on design or operational parameters affecting open rotor acoustics.

Research Approach

The literature review began with the historical background of open rotor research published in technical reports by the government and industry, articles in journals, and conferences papers. The literature review resulted in the identification of open rotor design parameters impacting the overall rotor noise. These parameters were broadly grouped in three categories: rotor design parameters, pylon installation parameters, and airframe integration parameters. For the sake of brevity, these parameters are detailed in Appendix A.

It was determined that the sensitivity study should focus on parameters dictating the rotor design. A preliminary list of parameters most likely to be used in the sensitivity study is presented in Table 1.

	Design Parameter	Remark
1	Diameter of front rotor	Noise levels reported to be sensitive to diameter of front rotor more than diameter of aft rotor, rotor spacing, and pitch angle of aft rotor
2	Pitch angle	Noise levels sensitive to pitch angle more than radius of aft rotor and rotor spacing, but less than diameter of front rotor.
3	Diameter of aft rotor	Noise levels sensitive to diameter of aft rotor more than rotor spacing, but less than diameter of front rotor and pitch angle.
4	Rotor spacing	Noise levels less sensitive to rotor spacing compared to diameters of rotors and pitch angle.
5	Blade stagger angle	Front rotor blade stagger angle was found to be an influential blade geometry parameter in a paper that studies optimization of 3D blade geometry for noise reduction.

6	Tip speed (Diameter and RPM)	Noise levels more sensitive to Aft tip speed than fore tip speed.
7	Aft rotor clipping	
8	Number of blades	
9	LE camber variable	Reduction of interaction between LE separation & Tip Vortex Interaction (Gen 1A)
10	Tip design in AFT rotor	reducing unsteady pressure, including incoming FWD rotor wakes (Gen 2A)

Milestone
A literature review report was completed, as summarized in Appendix A.

Major Accomplishments
The literature review resulted in a compilation of key findings from previous research studies, which aided in shortlisting the key parameters for the sensitivity study.

Publications
None

Outreach Efforts
None

Awards
None

Student Involvement
For this task, the graduate students worked in three design parameter groups, as described in Appendix A.

1. Rotor-only noise-related parameters: Chris Roper (continuing PhD student) and Mariam Emara (continuing PhD student)
2. Rotor–pylon flow-field interaction-related parameters: Brenton Willier (continuing PhD student)
3. Rotor–airframe flow-field interaction-related parameters: Maxime Varoqui (MS student)

Plans for Next Period
This task has been completed.

Task 2 - Parametric CAD Model Creation
Georgia Institute of Technology

Objective(s)
This task is focused on the development of a fully parametric CAD model of the open rotor and pylon configuration. This parametric model aids in mapping the independent parameters of the sensitivity study to a particular open rotor design geometry, which will later be used for computational aeroacoustics.

Research Approach

Under this task, a fully parametric model of the baseline geometry of the CROR and pylon configuration was generated. Emphasis was placed on ensuring that the resulting geometry is an accurate representation of the physical design of the reference blade set and is suitable for computational fluid dynamics (CFD) mesh generation. A scripting language was used to automate the model update based on a design point. This step is typically time-consuming because the mapping must be sufficiently robust such that design variable instances do not lead to a geometry with undesirable imperfections such as wrinkles or open surfaces that might be unsuitable for CFD analysis.

The initial geometry of the blades and nacelle was extracted from historical F31/A31 data provided by GE. Export-restricted files were provided, and key files among this group included 3D blade models, two-dimensional (2D) blade stations, and a test nacelle flow path. The parametric geometry model was recreated in Engineering Sketch Pad (ESP), an open-source, script-based, multidisciplinary design analysis & optimization (MDAO)-friendly CAD tool chosen because of its platform-independent framework, which is especially useful for cluster use during future sensitivity/MDAO-type studies.

First, the provided data were used to recreate the nacelle based on a 2D spline in the form of data points. This spline was rotated around a predefined axis to create the nacelle surface. Upon verification with additional restricted documents, the rotor locations and aft flow path trimming were found to be consistent with the original geometry data. Starting with the provided IGES blade model, cross-sections were extracted using Star-CCM+ and a Java macro. Because this task is repetitive, a Java macro was developed for multiple cross-sections to efficiently complete this task. This step of the process outputs raw cross-section coordinates in multiple CSV files. Next, a Python script was used to post-process these raw cross-section coordinates to reformat the data for ESP import. To retain information about the original shape, a final CSV file is created, which includes the original XYZ coordinates of the LE and TE, section twist, and section chord. To efficiently parameterize the airfoil section, the class-function/shape-function transformation (CST)/Kulfan method is employed to describe the shape of an airfoil with very few variables. Next, a script in ESP reconstructs the sections using the CST coefficients. The models recreated with this process were compared with the original model, and the maximum surface deviations were found to be less than 1/10 mm. With this diagnostic, the accuracy of the reconstruction process was verified. Finally, a pylon was added to the model. This pylon was built with the parameters of a generic wing-like span, root chord, taper ratio, aspect ratio, sweep, and twist. The pylon shape can be altered by choosing any number of cross-sections and by specifying CST coefficients for each section.

Milestone

A fully parametric CAD model of the historical F31/A31 blade set was successfully created for CAA validation and future sensitivity/MDAO studies.

Major Accomplishments

A fully parametric CAD model of the historical F31/A31 blade set was successfully created for CAA validation and future sensitivity/MDAO studies.

Publications

None

Outreach Efforts

None

Awards

None

Student Involvement

For this task, Brenton Willier (continuing PhD student with U.S. person credentials) played a major role in parsing F31/A31 data provided by GE. Brenton Willier also worked on parameterization of the F31/A31 CAD model in ESP.

Plans for Next Period

This task has been completed.

Task 3 - Computational Aeroacoustics Validation

Georgia Institute of Technology

Objective(s)

This task is focused on validating our predictions from simulation analyses against available experimental data from an open rotor configuration to evaluate discrepancies between numerical simulations and experiments. This validation will indicate the level of adequacy of the adopted numerical approach for open rotor design.

Research Approach

For this validation, the experimental data used are from NASA (Stephens, 2014; Sree, 2015), carried out on the wind tunnel open rotor model based on the F31/A31 blades, whereas the numerical simulations are based on a combined approach consisting of the lattice Boltzmann method (LBM) for unsteady aerodynamics and the Ffowcs Williams–Hawking (FW-H) method for far-field aeroacoustics.

Validation case and experimental data

The geometry of interest is an open rotor based on a subscale model based on the F31/A31 blade set. Geometrical details are provided in Table 2.

Table 1. Subscale F31/A31 open rotor.

	Number and type of blades	Diameter
Front Rotor	12 / F31	0.66 m
Aft Rotor	10/ A31	0.63 m

The utilized experimental data are from NASA experiments (Stephens, 2014; Sree, 2015) on a low-speed wind tunnel (9 ft x 15 ft). These experiments focused on three conditions: scaled take-off (STO), nominal take-off (NTO) and approach (APP). Furthermore, several rotor speeds were tested with two different configurations, with and without a pylon. The rotor design speed was 6530 RPM, and the inlet Mach number was 0.2 for all experimental runs.

Acoustic data were recorded by 18 sideline microphones, located at an offset distance of 5 ft parallel to the axis of the open rotor wind tunnel model. With the axis of the WT model and the plane of the aft rotor as a reference, these microphones covered angles of 17.6˚–140˚, with angles lower than 90˚ located upstream and angles larger than 90˚ located downstream.

The present validation focuses on an NTO case at 85% rotor speed. An illustration and details for this case are provided in Figure 1 and Table 3, respectively.

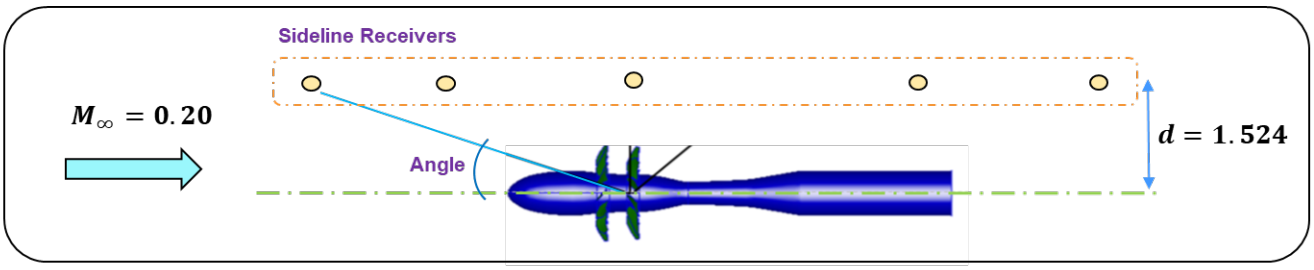

[*] Nark *et al.*, "Isolated Open Rotor Noise Prediction Assessment Using the F31A31 Historical Blade Set", AIAA paper 2016-1271

Figure 1. Validation case.

Table 2. Validation case details.

	Value	Unit
Mach number	0.2	
Rotor speed	5550.5	RPM
Blade pitch setting	40.1 front / 40.8 aft	degree
Angle of attack	0	degree

Numerical approach

The unsteady aerodynamic flow field is obtained by employing a commercial LBM solver, PowerFLOW. Unlike a traditional CFD solver that solves for macroscopic fluid quantities via Navier–Stokes equations, LBM-based solvers solve for microscopic particle distributions. Thus, modeling occurs at a level for which the physics are more fundamental. Such solvers exhibit low dissipation properties, rendering them suitable for aeroacoustic applications. Some details about the simulation setup are shown in Table 4.

Table 3. LBM simulation setup.

LBM Simulation	***Value***	***Remark***
Smallest spatial discretization	0.069 mm	At blade LE, TE, and tips
Time step	0.079 μs	
Mesh size	577 million	

Far-field aeroacoustics are calculated by employing an FW-H solver. This solver uses flow data recorded from unsteady simulations for a chosen surface. The surface is permeable surrounding the geometry of interest. The geometry is an open shell with an opening in the downstream end to avoid contamination from the open rotor wakes. The far-field acoustic receivers set to the FW-H solver are located at the same positions of the microphones in the experiments. Some details about the FW-H solver simulation are provided in Table 5.

Table 4. FW-H simulation setup.

FW-H Simulation	***Value***	***Remark***
FW-H spatial discretization	4.28 mm	Permeable surface
FW-H time step	7.5 μs	
Maximum frequency resolved	6.6 kHz	
Time for collecting flow data	4.5 revs.	Time for one revolution

Results

Numerical predictions of sound pressure level (SPL) at each rotor fundamental and first interaction, along with the overall sound pressure level (OASPL) as a function of the sideline geometrical angle, are shown in Figure 2. The rotor fundamentals are defined by the blade passage frequency, $BPF = nf_0$, where n is the number of blades and f_0 is the shaft frequency. The interaction frequencies are given by combinations of the blade passage frequencies of both the front and aft rotor, $m_1\, BPF_f + m_2\, BPF_A$, where m_1 and m_2 are integers; thus, the first interaction is given by $m_1 = m_2 = 1$. In the figure, both rotors exhibit maximum SPL values for geometric angles around their respective planes of rotation. The radiated noise, however, decreases significantly for upstream and downstream angles. In contrast, the SPLs for the first interaction are high for all angles despite

the presence of lobes in the directivity pattern. Finally, comparisons of the interaction noise with the OASPL directivity suggest that the interaction noise is dominant for the open rotor.

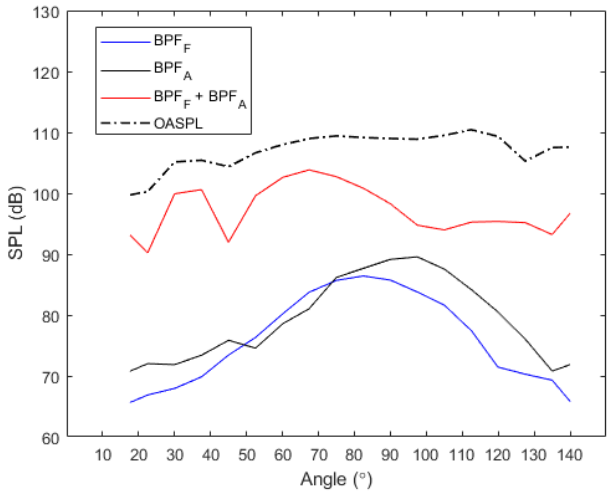

Figure 2. SPL at the fundamental frequencies (rotor and first interaction) and OASPL.

A comparison of the OASPLs from experiments (Sree, 2015) and numerical CAA simulations is shown in Figure 3. It is noted that the simulations exhibit better value agreement for intermediate angles, between 50° and 100°, whereas the agreement decreases for large upstream and downstream angles. Nevertheless, the trend of the OASPL from simulations resembles that of the experiments. Quantitatively, the OASPL from the CAA simulation has a root mean squared error (RMSE) – calculated across all sideline angles – of 4.5 dB.

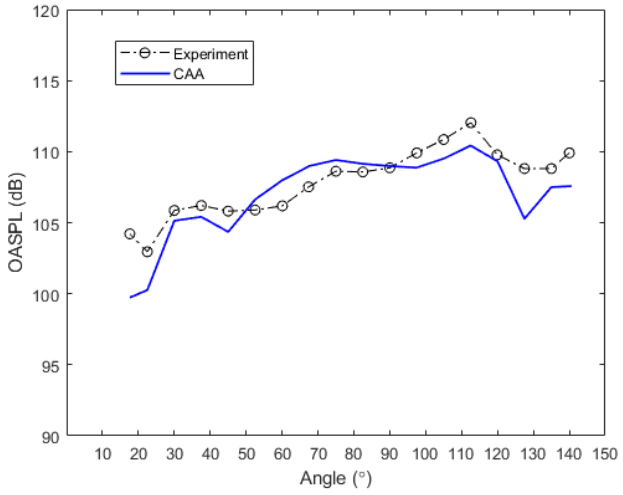

Figure 3. OASPL from simulations and experiments.

The overall power watt level (OAPWL) from the CAA simulation is compared with the experimental value in Table 6. The OAPWL calculation was performed exactly as described in the NASA report (Sree, 2015). For the case in consideration (NTO, 85% RPM_{DESIGN}, AoA=0), the resulting discrepancy is 1.75 dB.

Table 5. Comparison of OAPWLs.

Case	CAA	Experiment	Discrepancy
NTO, 85% RPM_{DESIGN}	125.75 dB	124 dB	1.75 dB

In summary, results obtained by our strategy of combined numerical simulations – LBM & FW-H – suggest good agreement with experimental data for one NTO case.

References

Sree, D. (2015). Far-field acoustic power level and performance analyses of F31/A31 open rotor model at simulated scaled takeoff, nominal takeoff, and approach conditions: Technical report I (Report No. CR 2015-218716). National Aeronautics and Space Administration.

Stephens, D. B. (2014). Data summary report for the open rotor propulsion rig equipped with F31/A31 rotor blades (Report No. TM 2014-216676). National Aeronautics and Space Administration.

Milestone(s)

None

Major Accomplishments

Initial validation of our numerical strategy for aeroacoustics was completed, exhibiting good agreement with experimental data for one case.

Publications

None

Outreach Efforts

None

Awards

None

Student Involvement

For this task, Brenton Willier (continuing PhD student with U.S. person credentials) worked on geometry preparation of the F31A31 open rotor and aerodynamics analysis.

Plans for Next Period

We and the sponsor have agreed to conduct further validations in the second year. However, these new validations will employ experimental data provided by the cost-share partner, GE. It must be pointed out that these data were not available during the first year of the project and were not yet accessible at the time of the writing of this report.

Appendix A: Summary Report of the Open Rotor Literature Review

Introduction

To achieve higher fuel efficiency, today's turbofan engines are becoming larger to house large fans and bypass ducts that accommodate higher volumes of bypass flow. However, as the size of a turbofan engine increases, drag and weight penalties eventually cancel the benefits of improved fuel efficiency [1]. To advance beyond these limitations, an open rotor engine concept is currently being investigated. An open rotor, also known as a 'Contra-Rotating Open Rotor (CROR)' or propfan, is an engine featuring a set of two propellers rotating in opposite directions. The propellers are driven by a gas turbine engine, which works on the same principle as a turbofan engine except that the engine core has no encompassing duct. Due to the unique counter-rotating fan design, the "bypass flow" of the air surrounding the engine core is qualitatively similar to the turbofan ducted flow, resulting in designs that obtain high bypass ratios without limiting the propeller fan size. It is estimated that open rotor engines currently prototyped in the industry achieve 30% reductions in fuel consumption compared with contemporary turbofan engines [2].

However, for open rotor engines, the absence of a noise-conditioning duct results in noise penalties due to complex aerodynamic interactions within the CROR system as well as between the system and surrounding installation components such as a pylon/fuselage. In particular, during take-off, an added effect of flow asymmetry introduces additional noise sources that magnify the emitted noise, resulting in challenges associated with strict noise certification standards. Therefore, noise improvements in CROR engines represent a primary challenge being addressed by engine manufacturers.

The main objective of this research is to perform a sensitivity study using high-fidelity Computational Aeroacoustic Analysis (CAA) to understand the impact of various CROR engine design parameters on overall noise performance, with the end goal of identifying key design parameters which future designers can target to meet noise-performance-related requirements. The sensitivity study will use the historical F31/A31 blade set as a baseline. Due to high computational costs, it is not feasible to evaluate all design parameters in this sensitivity study. Therefore, it is necessary to identify a subset of key design parameters based on experimental and computational studies previously performed by the community. In this report, we summarize key findings, primarily from the noise improvement perspective, that will guide the future course of the sensitivity study. Section A1 provides a brief historical background on open rotor technology. Section A2 presents an overview of CROR engine noise and a classification of CROR design parameters based on various noise sources. Section A3 provides a survey of design parameters and their impact on open rotor noise based on experimental and computational research outcomes published in the existing literature. This section also presents key parameters identified by the team as critical for the CAA-based sensitivity study that will be performed in years 2 and 3 of this effort.

A1. Historical Background

In the early 1980s, based on initial results of early NASA open rotor technology studies released to engine makers, GE initiated the historic *Unducted Fan (UDF)* program with full-scale development testing of UDF open rotor engines. Early efforts in UDF engine development aimed to overcome the increase in fuel prices caused by the 1973 Middle East oil embargo [3]. The UDF proof-of-concept testing consisted of three phases: scale model technology development through 2,500 hours of scale model testing in 1984, prototype engine development with 162 hours of ground testing in 1985, then 281 hours of flight testing on the Boeing 727-100 and the McDonnell-Douglas MD-80 aircraft in 1986 and 1987. The program led to the development and use of several model-scale facilities for testing open rotor technology, such as the GE Cell 41, NASA Glenn 9x15 Low-Speed Wind Tunnel, NASA Glenn 8x6 High-Speed Wind Tunnel, Boeing Transonic Wind Tunnel, and DNW Acoustic Wind Tunnel [4]. The blades selected for the UDF were of the F7A7 design, composed of advanced composite materials.

Extensive testing was aimed at understanding the aerodynamic and acoustic performance of the engine, and noise problems were quickly identified during the tests. Model-scale and full-scale results from the UDF program testing showed good comparisons, indicating that the model-scale tests could be projected to accurately estimate full-scale results. The UDF testing identified several noise mitigation methods such as increasing the number of blades, reducing the disk loading, applying aft rotor clipping, increasing the pylon–rotor distance, mitigating the pylon wake, and optimizing the rotor spacing, blade operation speed, and blade geometry [4]. In-flight tests showed that the UDF presented a 30% reduction in specific fuel consumption compared with a JT8D mounted on the other side of the Boeing 727 [5].

The technology development efforts were then used and leveraged to develop a GE36 engine for installation on the MD-91 and MD-92. The GE36 was designed to achieve nominal compliance with CAEP Chapter 4 requirements, with significant

improvement over previous UDF tests. The GE36 passed the test by featuring a cumulative margin of 10.5 dB with respect to Chapter 3 requirements. However, this achievement came with a reduction in aerodynamic performance, with a drop of 3% in cruise efficiency compared with a set that did not include the noise mitigation enhancements [4]. Despite this progress, as fuel prices fell after the embargo, the development costs could no longer be justified, and hence, the program was cancelled in 1989, halting any further development [3].

In the early 2000s, the environmental impact of the aviation industry and the need to explore efficient propulsion concepts led to a renewed interest in open rotor engines. From 2008 to 2012, as part of FAA's *Continuous Lower Energy, Emissions and Noise (CLEEN)* program and NASA's *Environmentally Responsible Aviation (ERA)* program, GE partnered with NASA to develop a mature open rotor engine aeroacoustic design. This *Modern Open Rotor Technology Development* program targeted a narrow body aircraft with a cruise Mach number of 0.78, leveraging CFD, CAA, and rig-scale testing to generate designs that achieved significant noise reductions well beyond what was attained in the 1980s while substantially retaining cruise performance. The blade designs included derivatives of the historical F31/A31 blade set, which was remanufactured and tested to provide a link back to data from the 1980s. The test program allowed for open rotor engine designs resulting in a 2%–3% improvement in overall propeller net efficiency over the best efficiency design of the 1980s while nominally achieving a noise margin of 15–17 EPNdB for Chapter 4 (when projected to full scale for a prescribed aircraft trajectory and installation) [4].

A2. Overview of Open Rotor Noise

Sound is a pressure wave that travels through matter by vibrations. A sound is characterized by its pitch and loudness, i.e., intensity. The pitch is perceived through the fundamental frequency of the noise, it describes the number of vibrations perceived per second. The range of audible frequencies for humans is 20 Hz to 20 kHz. The loudness or intensity of a noise is the energy carried by the wave, which is measured in decibels (dB). As shown in Figure 4, the energy of some noises is concentrated in specific frequencies or in a limited range of frequencies. This type of noise is called tonal or narrowband noise. Tonal noise is emitted by cyclic sources, such as rotating pieces like fans or compressors due to their blade thickness and blade loading [6]. The noise emission is repeated at each cycle, creating tonal noise at this specific cycle frequency. In contrast, the energy of other noise sources is spread across a large frequency spectrum, resulting in random and non-harmonic sound emission. This type of noise is called broadband noise. Turbulence in the flow due to complex interactions results in such noise [7][8]. Various noise sources associated with the complex flow field around an open rotor engine are shown in Figure 5.

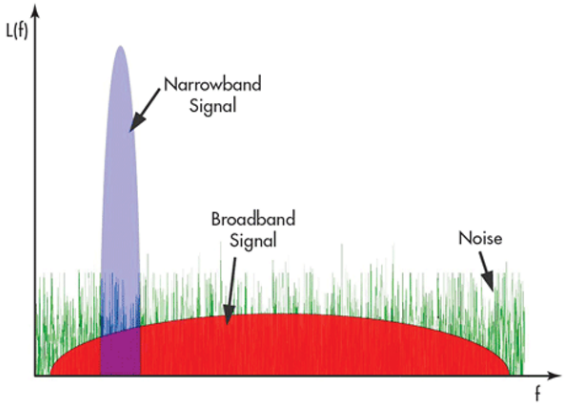

Figure 4. Noise power as a function of frequency for broadband and tonal noise (source: mwrf.com).

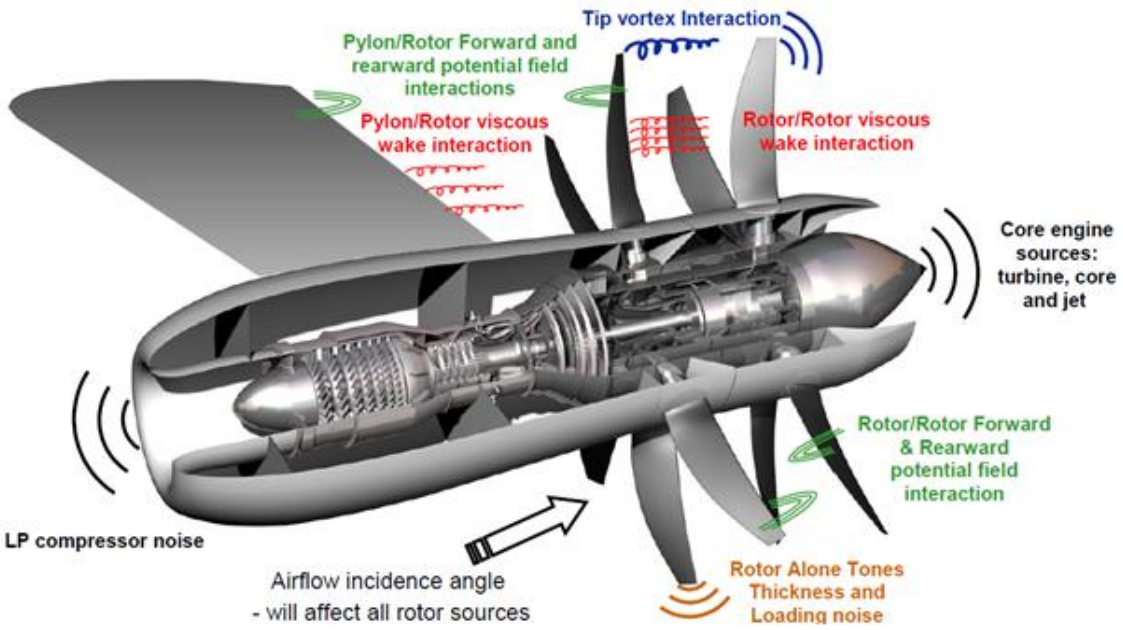

Figure 5. Open rotor noise sources. [8]

A3. Summary of Open Rotor Design Parameters and Their Impact on Noise

For the literature review, open rotor design parameters were divided into three primary groups based on the noise source:

1. Noise due to the rotor alone
2. Noise due to engine installation effects from rotor–pylon interactions
3. Noise due to engine installation effects from engine–airframe interactions

The rotor-blade-alone group involves rotor blade design parameters that contribute to the noise; examples of these parameters include the shape and number of the blades and the distance between the two rotors. Pylon installation effects include the parameters that define the pylon shape and position with respect to the rotor system. Finally, the airframe integration parameters include the engine location and aircraft configuration.

1. **Rotor-alone parameters**
   The main rotor parameters studied in the experimental campaign by NASA and GE were the spacing between the front and aft rotors, rotor diameters, aft rotor clipping, disk loading, blade count, tip speed, and pitch angle. Most of these parameters were identified as potential noise mitigation sources from the *UDF* program testing and *Modern Open Rotor Technology Development* program studies. Here, we summarize the impact of each of these design parameters as found in the literature.

   Aft rotor clipping: Decreasing the aft rotor diameter relative to the front rotor is called blade clipping, which is defined by the distance between the front rotor tip streamline and the aft rotor tip (Figure 6). Aft rotor clipping decreases the noise level by weakening the effect of the front rotor tip vortex interaction on the aft rotor: a clipping of 5% decreased noise levels for the F31/A31-based engine [9].

   Disk loading: Disk loading is defined as the power per unit propeller annulus area. It was observed that decreasing this parameter by adjusting other design parameters could significantly reduce noise levels. By increasing the rotor diameter of the F31/A31-based engine, disk loading was reduced from 100 hp/ft^2 to 59 hp/ft^2 to reduce noise levels [9].

Rotor diameter (R1 and R2): The noise levels were found to be more sensitive to the front rotor diameter than the aft rotor diameter, as well as other design parameters such as rotor spacing and the pitch angle of the aft rotor[10] [11]. In most studies, increasing the rotor diameter from the baseline led to lower noise levels due to a decrease in disk loading. The rotor diameter of the F31/A31-based engine was increased from 10.7 ft to 14 ft to decrease the noise level, which also provided net efficiency gains but increased weight and installation penalties [9]. In contrast, in a study focusing on the wake rather than the blade–vortex interaction, the radii of both rotors were decreased to reduce noise, with the aft rotor radius being larger than the front rotor radius to create a smaller wake area from the front rotor [11].

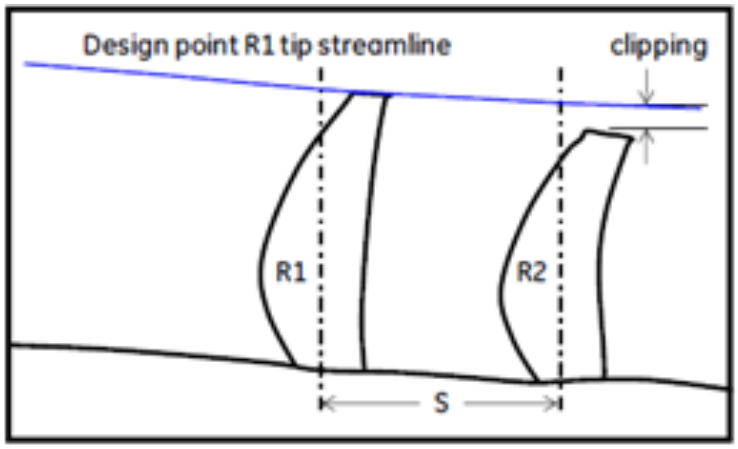

Figure 6. Main rotor parameters [4].

Pitch angle: In an optimization study conducted by the German Aerospace Center, DLR, for an 8x8 CROR engine, changing the pitch angle of the aft rotor by 2˚ from the baseline was found to reduce noise levels [11]. The noise level was also found to be more sensitive to pitch angle than the aft rotor radius or rotor spacing [10]. The variable blade pitch mechanism on the F31/A31-based engine allows the tip rotation speed to be adjusted for a given thrust and operating condition [9].

Tip speed: The tip speed or rotational speed of the rotors affects noise and can be adjusted by changing the pitch settings, where decreasing the pitch (increasing the blade setting angle) corresponds to increased RPM. A lower design tip speed reduces friction losses and brings the design lift coefficients closer to their optimum values but results in higher induced losses as a result of the stronger tip vortices [9]. Increasing the tip speed of the fore rotor at low flight speed was found to reduce noise in some historical experimental studies [9]. However, recent CFD study results on an SR2 blade geometry showed that noise can be reduced by decreasing tip speed [12]. Additionally, noise levels were found to be more sensitive to aft tip speed than fore tip speed. The effect of increasing tip speed was also found to be more significant for cases in which the forward blade count was greater than the aft blade count [12]. Another CFD study on a DLR CROR configuration showed that increasing the rotational speed of the aft rotor from approximately 926 to 1132 RPM led to high blade loading in the rear rotor, which increased the SPL from 142 to 153 dB [13].

Number of blades: Increasing the blade count relative to the baseline decreases the noise level due to the reduced loading per blade, which reduces induced losses as well as loading and rotor–rotor interaction noise [9]. Additionally, historical test data from the UDF program showed that mismatched front and aft blade counts significantly affect noise and rotor interaction tones [9]. A CFD study on an SR2 blade geometry showed that the difference in EPNL between the lowest noise level combination (12*15) and highest noise level combination (8*5) of blade counts was approximately 35 dB (EPNL) [12].

Blade design: The design of the blade or planform variables also affect noise levels. Examples of blade parameters include the twist angle and chord length for different design sections, the tip shape or leading edge, and the blade thickness. For example, Gen 2A+B of the F31/A31 blade was designed to reduce the contribution of rotor–rotor interaction noise of the forward rotor tip vortex relative to its wake [9]. A CFD study focused on planform design parameters of the aft rotor of a NASA SR-7L geometry found that the other rotor parameters, such as blade diameters and rotor spacing, showed a more significant effect on noise. In that study, the chord length, twist angles at several

radial locations, and leading-edge coordinate of the tip section were considered as planform design parameters, and the optimized configuration showed a noise reduction of 0.6 dB [14].

Blade stagger angle: The blade stagger angle is a design parameter defined as the angle between the chord line of the blade and the rotor axial direction at different cross-sections of the blade. The front rotor blade stagger angle, which affects the radial load distribution was found to be influential in an optimization study of three-dimensional blade geometry for noise reduction [15].

Rotor-rotor spacing (S): The rotor-rotor spacing is the distance between the forward and aft rotors. This distance can be measured with respect to the pitch change axes or with respect to the aft-most point of the front rotor and the forward-most point of the aft rotor. Propeller noise is exacerbated by the effects of incoming unsteady flow and loading on the individual blades. Increasing the rotor spacing allows turbulent structures emitted from the front rotor to weaken before interacting with the aft rotor, resulting in reduced noise levels [9] [16]. A study on the effect of axial spacing between rotors showed that increasing the spacing by 46% led to a reduction of the total SPL by approximately 3 dB [17].

2. Design parameters related to rotor-pylon flow-field interactions

In the aft configuration, the wake of the support pylon causes unsteady loading on the front rotor. The literature review showed that multiple configurations have been tested to evaluate the sensitivity of these interactions. An isolated rotor is often used as a baseline for overall noise and interaction tones. Then, a pylon is added upstream of the rotor to evaluate the effect of the pylon wake on the overall noise. Finally, a fuselage and empennage are added to the flow field. With these different configurations, multiple parameters can be varied to uncover the sensitivities with respect to the produced noise.

Fuselage-rotor (tip) spacing: The fuselage-tip spacing is the minimum radial distance between the tip of the blade path and the fuselage. It was found that the noise decreases as the fuselage-tip distance increases [18].

Pylon-rotor spacing: The pylon-rotor spacing is the distance between the trailing edge of the pylon and the forward-most point of the front blade. The front rotor ingests the wake produced by the pylon, and this unsteady loading increases noise. It was found that noise decreases as the pylon-rotor spacing is increased [18] [19].

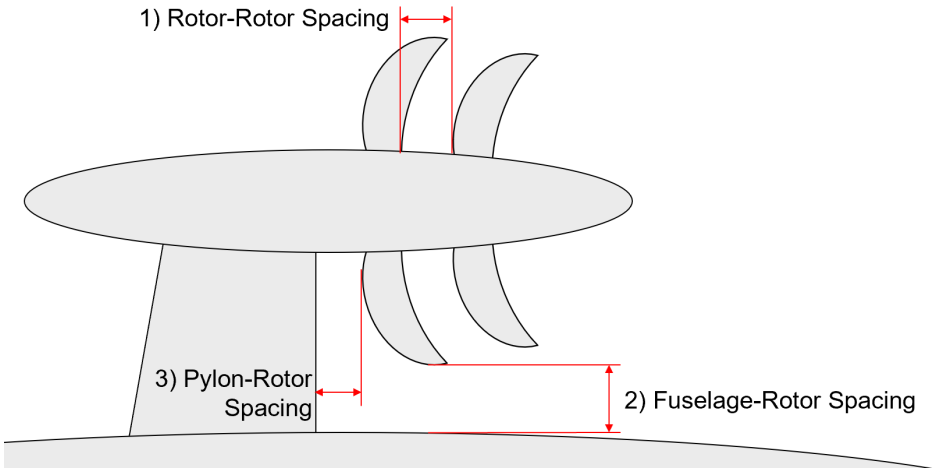

Figure 7. Rotor installation parameters.

Pylon angle of attack: The angle of attack of the pylon was examined because at takeoff, when noise is of high concern, the pylon would be at a high angle of attack. The angle of attack of the pylon was found to have no apparent trend applicable to consistent noise reduction between -5° and +5° [18]. Further work is required to understand the effect of the angle of attack on the pylon wake and resulting noise.

Pylon sweep: Adding a sweep angle to the pylon was found to reduce noise compared with a straight pylon [19]. This was specifically a binary comparison between a straight and swept pylon. Optimal sweep angle will depend on the pylon and rotor geometries and other installation parameters.

Based on these parameter evaluations, the front rotor was found to be the source of noise changes. The aft rotor and interactions, for the most part, remained constant. It has been found that emitted noise due to pylon wake interaction is skewed towards the pylon [20]. This skew is more apparent during cruise than during take-off (Figure8) [20].

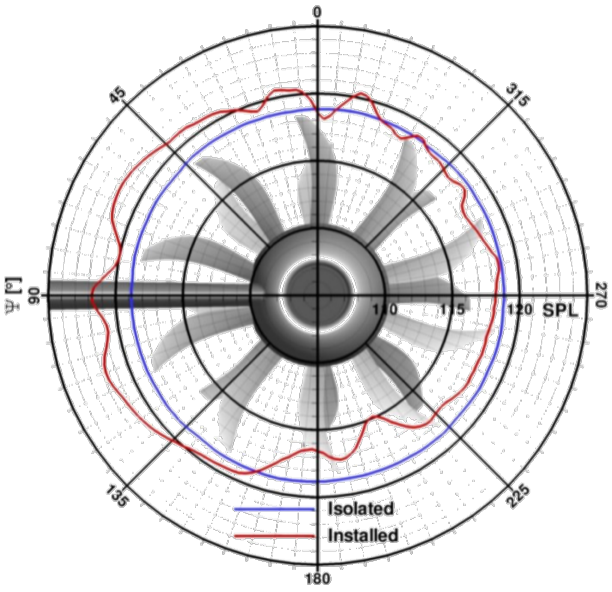

Figure 8. Noise directivity is skewed toward the pylon [20]

In summary, the literature review suggests that addition of the pylon results in increase in noise by at least 10dB [19] [18]. The addition of a fuselage and empennage results in an additional noise increase of 2–3 dB compared with the pylon-only configuration [18].

Technology infusion: pylon trailing-edge blowing

One possible technology infusion that could be applied to reduce pylon-induced noise is pylon trailing-edge blowing. In an attempt to fill the pylon wake, a blower can be added to the trailing edge of the pylon, as shown in Figure 9.

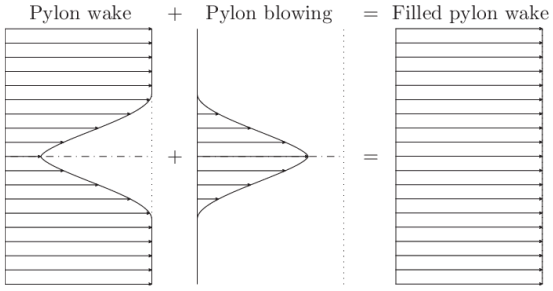

Figure 9. Notional filled pylon wake [21].

The blown flow is injected at a velocity slightly higher than the free stream, using the general physical test setup shown in Figure 10.

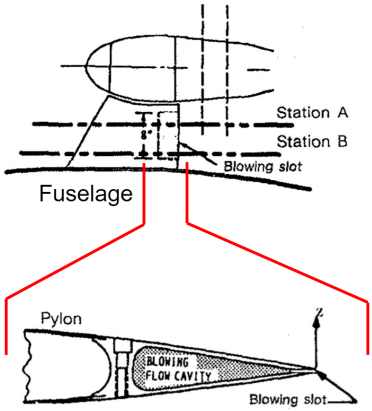

Figure 10. Pylon TE blowing schematic. [18]

The testing performed in the literature found that pylon blowing reduced the velocity deficit in the pylon wake; however, this mitigation did not reduce the overall wake width. Promisingly, noise due to the pylon wake was reduced, although the interaction tones were unchanged. If this technology is to be considered, further work should focus on exploring trends for varying blowing rates, angles of attack, and freestream velocities. The flow mixing should also be optimized. Finally, the flow near the fuselage should be optimized to encourage a smooth flow to avoid exacerbating fuselage-tip-induced noise [18][19][21].

3. Design parameters related to open rotor engine–airframe integration

As discussed earlier, the interaction of the rotor flow field with the airframe results in additional noise that must be considered. Design considerations related to airframe integration must include the position of the engine with respect to the airframe and the aircraft shape. Because this study is primarily focused on open rotor applications for narrow-body single-aisle aircrafts, the literature review was limited to traditional tube and wing airframes, excluding other unconventional structures, such as blended wing body aircrafts. For engine–airframe integration, the engine mounting location is an important factor. First, we will consider tail-mounted configurations and their impact on noise shielding.

Tail configuration comparison

The three main configurations considered are the U-Tail, the T-Tail, and the L-Tail (Figure 11). In traditional aircraft designs, the L-tail configuration is most common. However, the UDF flight tests on the Boeing 727 [22] in 1986 and the MD-80 in 1987 featured a T-tail configuration [23]. After renewed interest in open rotor engines, new programs studied the L-tail and U-tail configurations in addition to the original T-tail used by the UDF programs at the end of the 1980s.

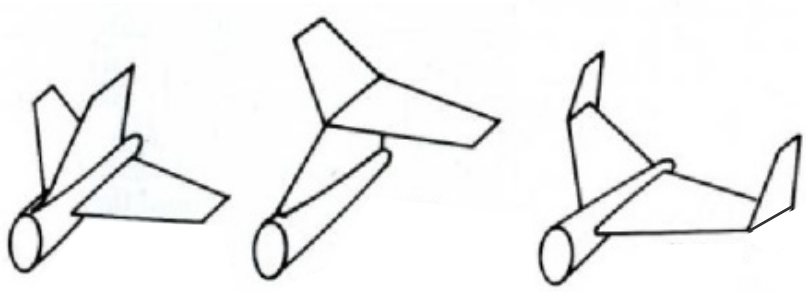

Figure 11. From left to right, L-tail, T-tail, and U-tail configurations. [24]

The WENEMOR project (2011–2013) was a European Clean Sky Joint Technology Initiative to investigate aero-acoustic noise emission measures for advanced regional open rotor A/C configurations. The engine used for this project was a 1:7-scale modular model with interchangeable tails, pylon elongations and angles, and variable angle of attacks. The blade profiles

were designed by SAFRAN and featured 12 blades for both the front and aft propellers. Experiments were performed for a total of 16 different configurations in this program for both approach and takeoff certification points. The engine was in pusher mode for nine of the configurations and in tractor mode for seven configurations. The open rotor pylon length was 522 mm and was set with an angle of 42°. The parameters that were varied were the angle of attack, flow speed, and tail shape (T-, U-, or L-tail). The noise calculations were recorded as the difference in OASPL, relative to a baseline case with an 8° angle of attack and a flow speed of 24m/s. The noise was measured by a far-field microphone array.

According to data analyses from this project [25] [26], L- and U-tails performed better, with a globally more significant shielding than the T-tail configuration. The largest noise reduction came from the PS-E engine configuration (Figure 12), which contained an open rotor in pusher mode mounted on a 42-degree and 1.04D long pylon. The comparison between the L- and U-tails was very close in terms of advantages and disadvantages. The L-tail in the PS-E configuration yielded better results for the OASPL, but the U-tail led to higher noise reductions for broadband and tonal noise for the takeoff certification configuration. None of the configurations studied outperformed the others for all harmonics under both takeoff and approach conditions.

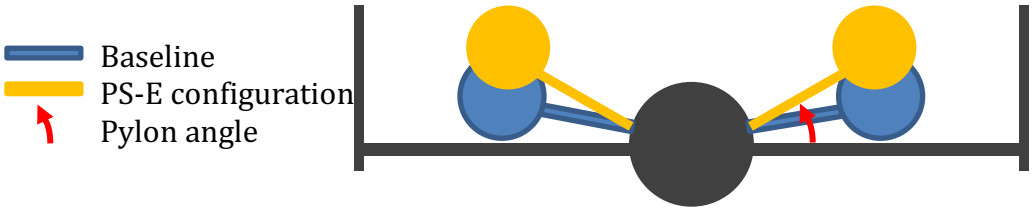

Figure 12. PS-E configuration for a U-tail airframe.

The influence of tail type has also been discussed in another previous work [27]. In that study, the L- and U-tails were compared with a T-tail baseline. An angle of attack of 6° mounted on a U-tail seemed to yield the best results among the configurations studied, presenting a noise reduction in almost every direction, except for $\sim \pm 10°$ with respect to the vertical axis.

Another CFD study [28] compared the effects of L-tail, U-tail, and T-tail configurations on the EPNL for two takeoff certification points: flyover and lateral. This study considered an open rotor engine for which the pylon planform, nacelle contour, and rotor position were approximated from the SAFRAN Aircraft Engines CROR model. The CROR was mounted in pusher mode and featured 12 blades (14-ft diameter) in front and 10 in aft position. The CROR rotor located on the tail of the aircraft with a pylon inclined by 45° in the downward direction showed a noise attenuation of 7 dB for the L- and U-tails in the aft downward direction. This reduction was attributed to the relative position of the horizontal tail below the engine, which allowed an upward noise reflection. Yet, this attenuation was compensated in the aft upward direction by a noise level increase for these two tails with respect to the no-tail and T-tail configurations. The behavior of the U-tail in the vertical plane was similar to that of the L-tail, as the geometries of the horizontal stabilizers for both tails are similar. The T-tail exhibited the opposite behavior because of its symmetric geometry: the attenuation was observed for the aft upward area and the noise increase was observed in the aft downward area. The effect of the engine axial position alongside an axis parallel to the flight was also studied. For the lateral certification point, the study underlined a global compensation of reflection and shielding effects for all configurations. The directivity and noise intensity for all tails studied were similar to those for the no-tail case. Thus, none of the three tail configurations induced a significant change for lateral observers.

However, in flyover, the T-tail produced higher noise regardless of the engine axial position, with minor improvements for a forward engine placement. The zero location for this study corresponds to the CROR midplane aligned with the tail leading edge. Even though the U-tail and T-tail configurations featured similar behaviors, an optimum position was found for the U-tail at a position of 2 m aft of the leading edge. For this set, the attenuation relative to the case without a tail was -2.4 EPNdB.

Wing- or U-tail-mounted CROR

Thus far, our interest has focused on tail configurations for the airframe integration. However, another study [29] compared the benefits of a wing-mounted versus a tail-mounted CROR. The geometry considered for this study was the demonstrator rotor of the UDF program, geared with eight F7A7 blades for each rotor. The pitch angles of the blades tested here were 30.8° and 31.6° for static conditions and reached 38.0° and 37.2° for Mach numbers higher than 0.2. However, the pylon was not attached to the airframe; rather, it was positioned relative to the wing or the tail.

Figure 13. Over-wing and U-tail experimental installation. [29]

For a U-tail installation with the rotor center aligned with the leading edge of the U-tail, significant shielding of up to 20 dB in the rotor tone was observed for emission angles of approximately 60°–120°. When the rotor was positioned in front of the main wing, the presence of the wing in the wake of the rotor caused flow distortions, and the noise increased by 10 dB. Unlike the latter case, the results showed a reduction of 10 dB in broadband noise when the open rotor was placed right above the main wing. All the measurements were compared relative to the isolated rotor case.

Another way to simulate the behavior of a wing or tail configuration in lateral directions is by using a wall. Two studies [30] [31] reported on this type of wall-shielding experiment. The effect of noise shielding was tested on two different wall lengths and two different positions (Figure 14). A long wall simulated a large wing while a short wall represented a U-tail configuration. The open rotor considered was the historical GE F31/A31 blade set. A microphone array was set up to record the emitted noise. It was concluded that all barriers produced an attenuation of nearly 10 dB, irrespective of their position or length. However, a diffraction phenomenon was observed along the edges of the short wall. Thus, a larger barrier wall corresponds to better noise reduction.

An investigation on the positions of the short wall with respect to the center of the CROR was also performed [31]. The wall in the forward position featured a cumulative reduction of almost 3 EPNdB for approach, lateral, and flyover conditions, whereas the aft position induced an EPNL benefit of 8.3 EPNLdB. Hence, the aft position was found to be more suitable for noise reduction. However, the authors suggested that the results may be slightly exaggerated due to the small facilities in which the experiment was conducted; hence, these results should be used as validation measures for more accurate tests.

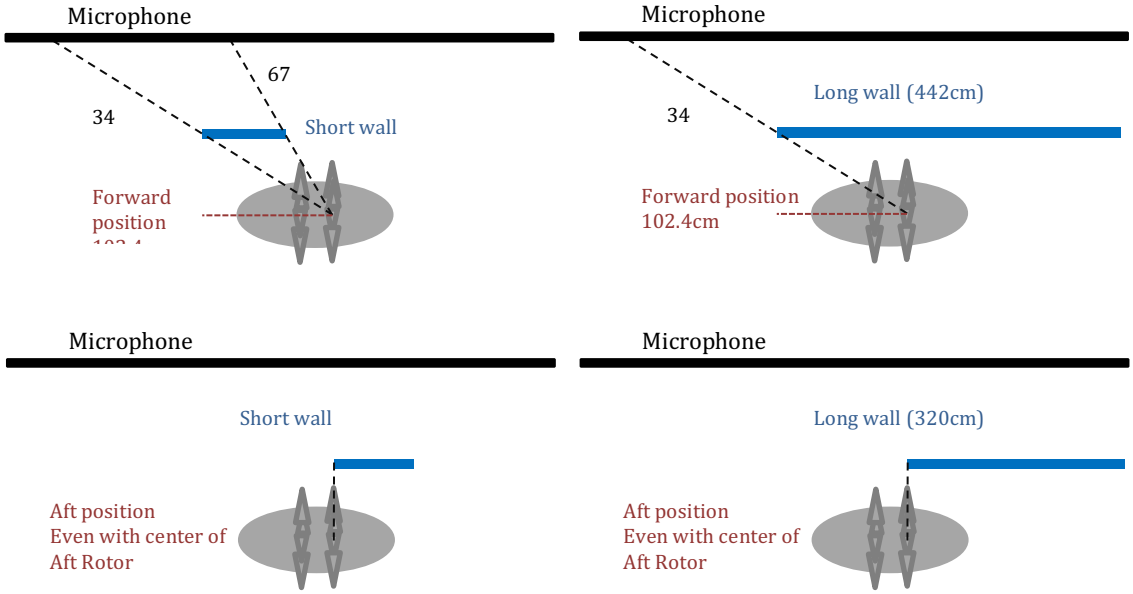

Figure 14. Illustration of the F31/A31 open rotor tested with barrier walls in the forward and aft positions.

BIBLIOGRAPHY

[1] L. S. Langston, "Open Rotor Engines—Still an Open Question?," *ASME. Mechanical Engineering.* , December 2018.

[2] SAFRAN-GROUP, "Safran celebrates successful start of Open Rotor demonstrator tests on new open-air test rig in southern France," October 2017. [Online]. Available: https://www.safran-group.com/media/safran-celebrates-successful-start-open-rotor-demonstrator-tests-new-open-air-test-rig-southern-france-20171003.

[3] Smithsonian National Air and Space Museum, "General Electric GE36 Unducted Fan (UDF) Turboprop Engine," [Online]. Available: https://airandspace.si.edu/collection-objects/general-electric-ge36-unducted-fan-udf-turboprop-engine/nasm_A19920001000.

[4] FAA, General Electric, "Open Rotor Engine Aeroacoustic Technology Final Report," 2014.

[5] M. McCarthy, "Contra-rotating Open Rotor Reverse Thrust Aerodynamics," Cranfield University, 2011.

[6] NoiseNews, "Tonal Noise Analysis with Optimus Green Sound Level Meters," 2017.

[7] S. Glegg and W. Devenport, Aeroacoustics of Low Mach Number Flows, Vols. Chapter 16 - Open rotor noise, 2017, pp. 399-436.

[8] KAIST Aeroacoustics Lab, "Flow and Acoustics of Turbo Jet and Rocket," [Online]. Available: https://sites.google.com/site/aeac1234/applications/hydraulic-power.

[9] FAA, General Electric, "Open Rotor Engine Aeroacoustic Technology Final Report," 2014.

[10] J.-S. Jang, S. Choi, H.-I. Kwon, D.-K. Im, D.-J. Lee and J.-H. Kwon, "A Preliminary Study of Open Rotor Desing Using a Harmonic Balance Method," in *50th AIAA Aerospace Sciences Meeting Including the Horizons Forum and Aerospace Exposition*, 2012.

[11] H. Kwon, S. Choi, J.-H. Kwon and D. Lee, "Surrogate-Based Robust Optimization and Design to Unsteady Low-Noise Open Rotors," *Journal of Aircraft,* 2016.

[12] D. A. Smith, A. Filippone and N. Bodjo, "A Parametric Study of Open Rotor Noise," in *25th AIAA/CAES Aeroacoustics Conference*, 2019.

[13] S. Yi, H.-I. Kwon, D. Im, S. Choi, M. Park and D.-J. Lee, "Parameter Study of Low Noise CROR System," in *34th AIAA Applied Aerodynamics Conference*, 2016.

[14] H.-I. Kwon, S.-g. Yi, S. Choi, D.-J. Lee, J.-H. Kwon and D.-K. Im, "Design of a Low-Noise Open Rotor Using an Implicit Harmonic Balance Method," in *51st AIAA Aerospace Sciences Meeting*, 2013.

[15] R. Schnell, J. Yin, C. Voss and E. Nicke, "Assessment and Optimization of the Aerodynamic and Acoustic Characteristics of a Counter Rotating Open Rotor," in *ASME Turbo Expo*, 2010.

[16] B. A. Janardan and P. R. Gliebe, "Acoustic characteristics of counterrotating unducted fans from modelscale tests," *Journal of aircraft,* vol. 27, no. 3, 1990.

[17] P. A. Moshkov, V. Samokhin and A. Yakovlev, "Problem of the Community Noise Reduction for Aircraft with Open Rotor Engines," *Russian Aeronautics Vol. 61 No. 4,* pp. 647-650, 2018.

[18] B. Shivashankara, D. Johnson and R. Cuthbertson, "Installation Effection on Counter Rotation Propeller Noise," *AIAA,* 1990.

[19] J. Ricouard, E. Julliard and et al, "Installation effects on contra-rotating open rotor noise," *16th AIAA/CEAS aeroacoustics conference,* 2010.

[20] A. Stuermer and Y. Jianping, "Aerodynamic and aeroacoustic installation effects for pusher-configuration CROR propulsion systems," *28th AIAA Applied Aerodynamics Conference,* 2010.

[21] T. Sinnige and L. L. M. Veldhuis, "Pylon Trailing Edge Blowing Effects on the Performance and Noise Production of a Pusher Propeller," 2014.

[22] R. W. Harris and R. Cuthbertson, "UDF/727 Flight Test Program," in *AIAA/SAE/ASME/ASEE 23rd Joint Propulsion Conference*, San Diego, CA, 1987.

[23] H. Nichols, "UDF engine/MD80 flight test program," in *AIAA/SAE/ASME/ASEE 24th Joint Propulsion Conference*, Boston, Mass., 1988.

[24] J. Dansie, "What should my tail look like?," HMFC, 2018. [Online]. Available: http://www.hmfc.com.au/index.php/ground-school/what-should-my-tail-look-like. [Accessed 07 2021].

[25] J. Kennedy, P. Eret and G. Bennett, "A parametric study of airframe effects on the noise emission from installed contra-rotating open rotors," *International Journal of Aeroacoustics,* 2018.

[26] L. Sanders, D. C. Mincu, P. L. Vitagliano, M. Minervino, J. Kennedy and G. Bennett, "Prediction of the acoustic shielding by aircraft empennage for contra-rotating open rotors," *International Journal of Aeroacoustics,* pp. 626-648, 2017.

[27] J. Kennedy, P. Eret and G. Bennett, "A parametric study of installed counter rotating open rotors," in *19th AIAA/CEAS Aeroacoustics Conference*, Berlin, Germany, 2013.

[28] L. Dürrwächter, M. Keßler and E. Krämer, "Numerical Assessment of Open-Rotor Noise Shielding with a Coupled Approach," *AIAA Journal,* pp. 57(5), 1930-1940, 2019.

[29] M. Czech and R. H. Thomas, "Open Rotor Installed Aeroacoustic Testing with Conventional and Unconventional Airframes," in *19th AIAA/CEAS Aeroacoustics Conference*, Berlin, Germany, 2013.

[30] D. B. Stephens and E. Envia, "Acoustic Shielding for a Model Scale Counter-rotation Open Rotor," in *17th AIAA/CEAS Aeroacoustics Conference*, 2011.

[31] J. Berton, "Empennage Noise Shielding Benefits for an Open Rotor Transport," in *17th AIAA/CEAS Aeroacoustics Conference (32nd AIAA Aeroacoustics Conference)*, Portland, Oregon, 2011.

[32] S. Yi, H.-I. Kwon, D. Im, S. Choi, M. Park and D.-J. Lee, "Parameter Study of Low Noise CROR System," in *AIAA Aviation Forum - 34th AIAA Applied Aerodynamics Conference*, 2016.

[33] A. R. Stuart, "The Unducted Fan Engine," in *AIAA-85-1190*, 1985.

[34] E. S. Hendricks and M. T. Tong, "Performance and Weight Estimates for an Advanced Open Rotor Engine," in *AIAA-2012-3911*, 2012.

[35] E. Kravitz, "Analysis and Experimetns for Contra-Rotating Propeller," MIT, 2011.